Microwave studies of chaotic systems

Lecture 1: Currents and vortices

Hans-Jürgen Stöckmann

stoeckmann@physik.uni-marburg.de

Fachbereich Physik, Philipps-Universität Marburg, D-35032 Marburg, Germany

FOR760

Scattering systems with complex dynamics

Contents

- Billiard experiments
- Nodal domains
- Random superposition of plane waves
- Flows
- Freak waves
- Summary

Billiard Experiments

Why billiard systems?

They are one of the paradigms of non-linear dynamics!

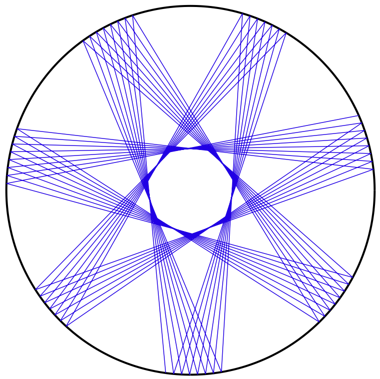

Circular billiard:

Two constants of motion (energy E, angular momentum L)

$\Longrightarrow$ The circular billiard is integrable!

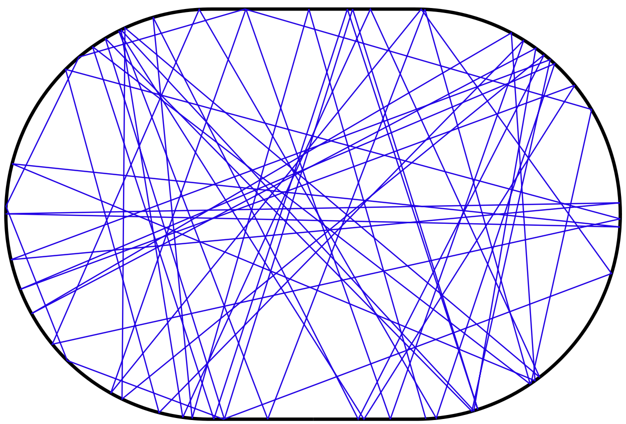

Stadium billiard:

One constant of motion (energy E)

$\Longrightarrow$ The stadium billard is chaotic!

Unique property of billiards

One-to-one correspondence between

- the stationary Schrödinger equation

$$-\frac{\hbar^2}{2m}\left(\frac{\partial^2}{\partial x^2}+\frac{\partial^2}{\partial y^2}\right)\psi_n = E_n\psi_n$$

  with the boundary condition $\psi_n|_R = 0$, and

- the Helmholtz equation

$$-\left(\frac{\partial^2}{\partial x^2}+\frac{\partial^2}{\partial y^2}\right)\psi_n = k_n^2\psi_n\,!$$

Possibility to study "quantum chaos" by means of classical waves!

Realizations

a) classical waves

- vibrating plates (Chladni 1787)
- microwave billiards (Stöckmann *et al.* 1990)
- capillary waves on water surfaces (Blümel *et al.* 1992)
- acoustic resonances in solids (Ellegaard *et al.* 1995)
- distorted light fibers (Doya *et al.* 2002)

b) quantum mechanical systems

- antidot structures (Weiss *et al.* 1991)
- mesoscopic billiards (Marcus *et al.* 1992)
- quantum corrals (Crommie *et al.* 1993)
- tunnelling barriers (Fromhold *et al.* 1994)

(For details see: *Quantum Chaos – An introduction*, H.-J. Stöckmann, Cambridge University Press 1999)

Microwave billiards

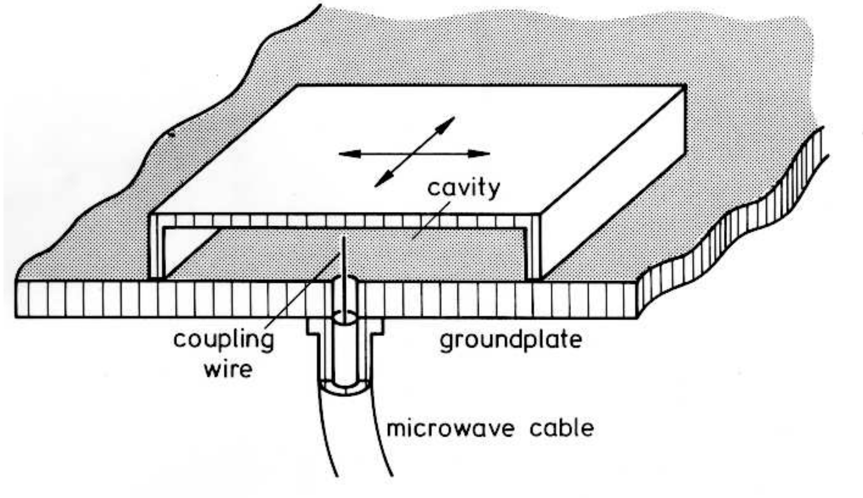

Typical set-up

Such a set-up is used by our students in their practical exercises.

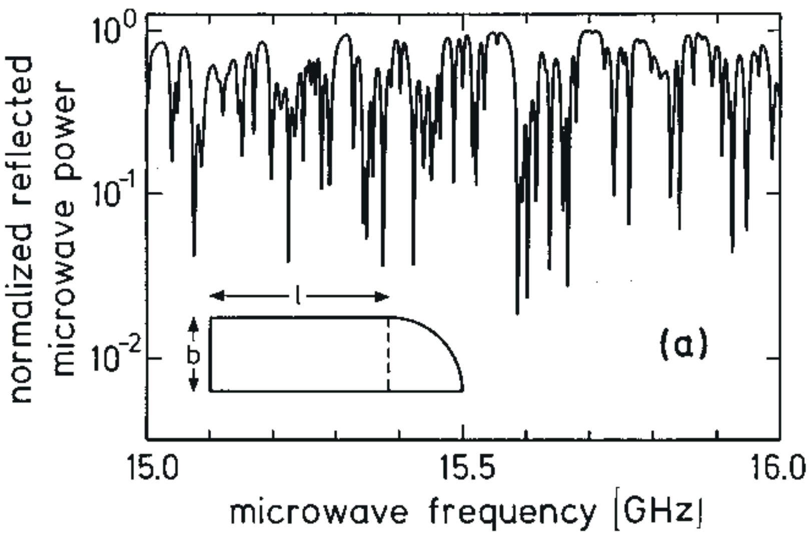

Reflection spectrum of a quarter-stadium billiard ($b = 20$ cm, $l = 36$ cm)

Scattering theory

Microwave experiments directly yield scattering matrix S (Stein *et al.* 1995):

- S_{ii}: reflection amplitude at antenna i
- $S_{ij}, (i \neq j)$: transmission amplitude between antennas i and j.

Billiard Breit-Wigner formula for isolated resonances:

$$S_{ij} = \delta_{ij} - 2\imath\gamma \sum_n \frac{\bar{\psi}_n(r)\bar{\psi}_n(r')}{E - E_n + \frac{\imath}{2}\Gamma_n}$$

$\Longrightarrow$ Complete Green function available, including

- spectra
- wave functions
- transport properties

Nodal domains

E. F. F. Chladni 1756 – 1827

Chladni, demonstrating the sound figures in the Palais of Thurn und Taxis, Regensburg 1800

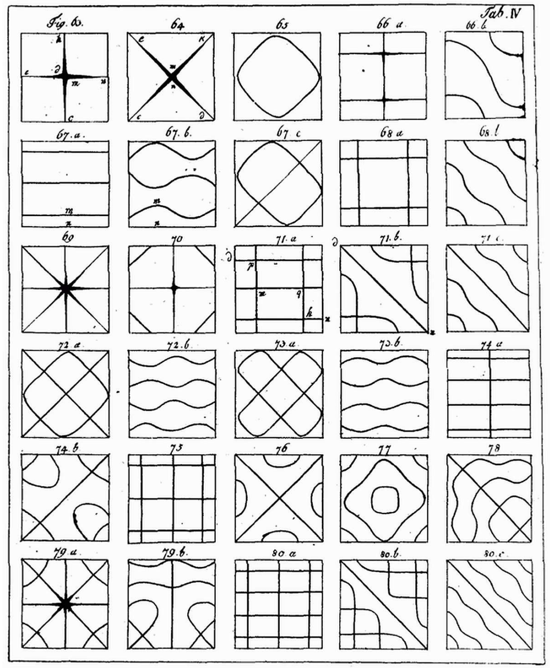

Sound figures (E. Chladni, *Akustik*, Leipzig 1802)

Chladni figures

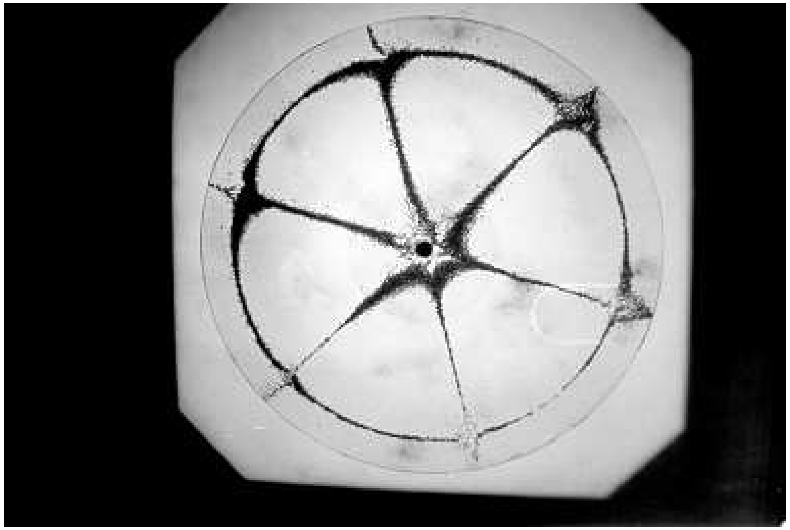

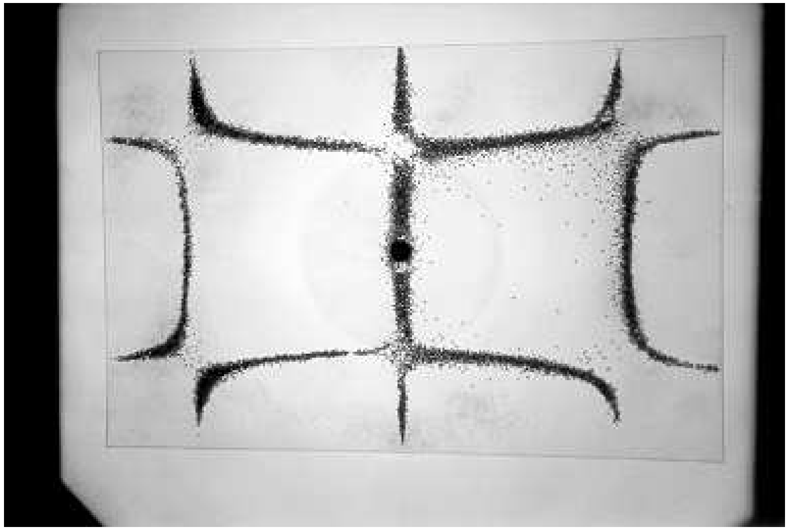

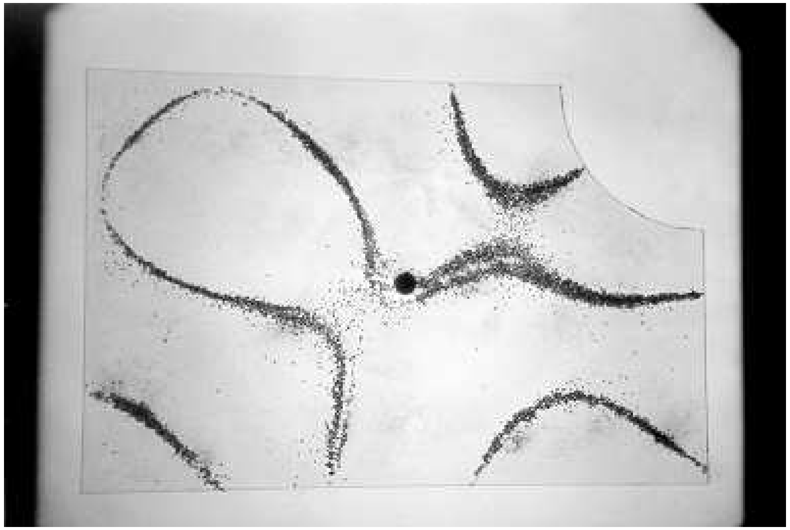

circular billiard: integrable

rectangular billiard: pseudo-integrable

Sinai-billiard: chaotic

Nodal domains statistics

VOLUME 88, NUMBER 11 PHYSICAL REVIEW LETTERS 18 MARCH 2002

Nodal Domains Statistics: A Criterion for Quantum Chaos

Galya Blum, Sven Gnutzmann, and Uzy Smilansky

Proposes nodal domain statistics to discriminate between integrable and chaotic systems.

Nodal domains statistics

VOLUME 88, NUMBER 11 PHYSICAL REVIEW LETTERS 18 MARCH 2002

Nodal Domains Statistics: A Criterion for Quantum Chaos

Galya Blum, Sven Gnutzmann, and Uzy Smilansky

Proposes nodal domain statistics to discriminate between integrable and chaotic systems.

VOLUME 88, NUMBER 11 PHYSICAL REVIEW LETTERS 18 MARCH 2002

Percolation Model for Nodal Domains of Chaotic Wave Functions

E. Bogomolny and C. Schmit

Expressions from a percolation model for mean number of nodal domains in dependence of eigenvalue number n, and related quantities.

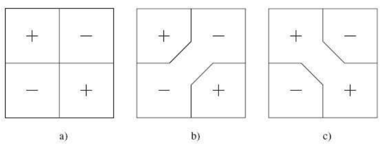

FIG. 2. (a) True nodal crossing. (b) and (c) Avoided nodal crossings.

Nodal lines and nodal points

In open systems: $|\psi|^2 = \psi_R^2 + \psi_I^2$

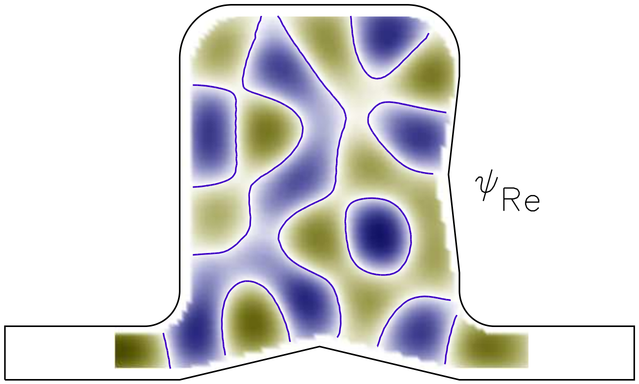

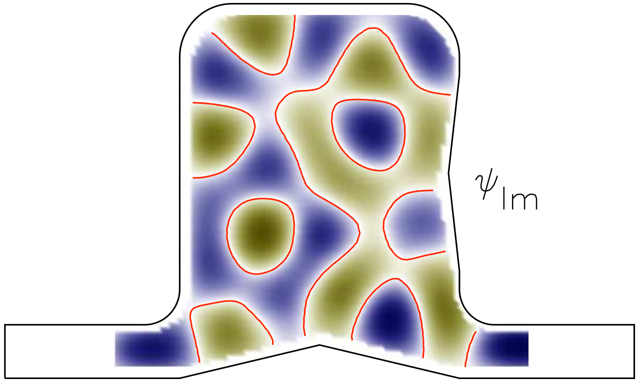

ψ_R, ψ_I: nodal lines

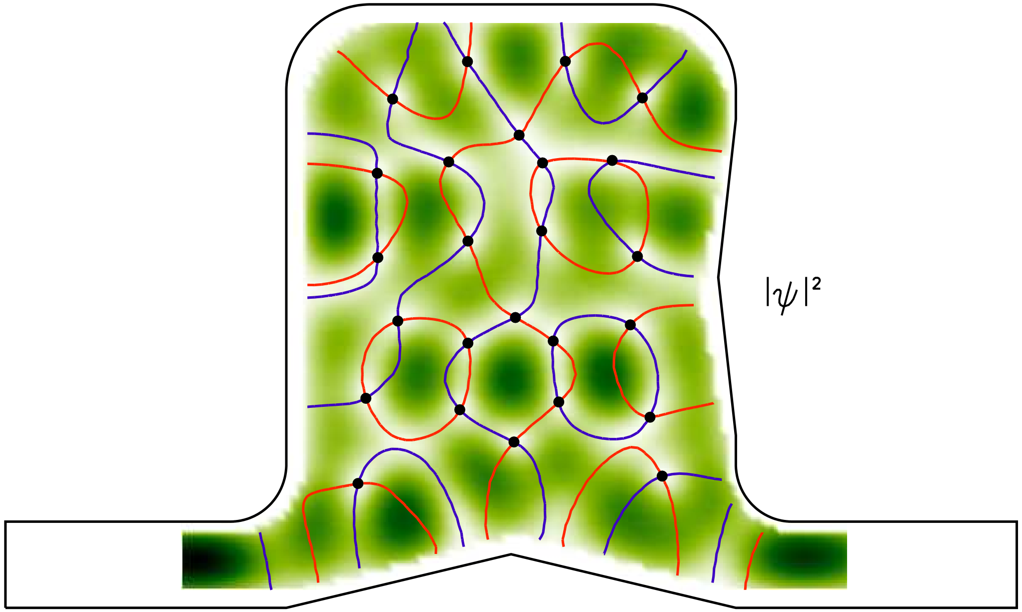

$|\psi|^2$: nodal points

Number of nodal domains

Prediction from percolation model: $\nu_n = an$, $a = 0.062$

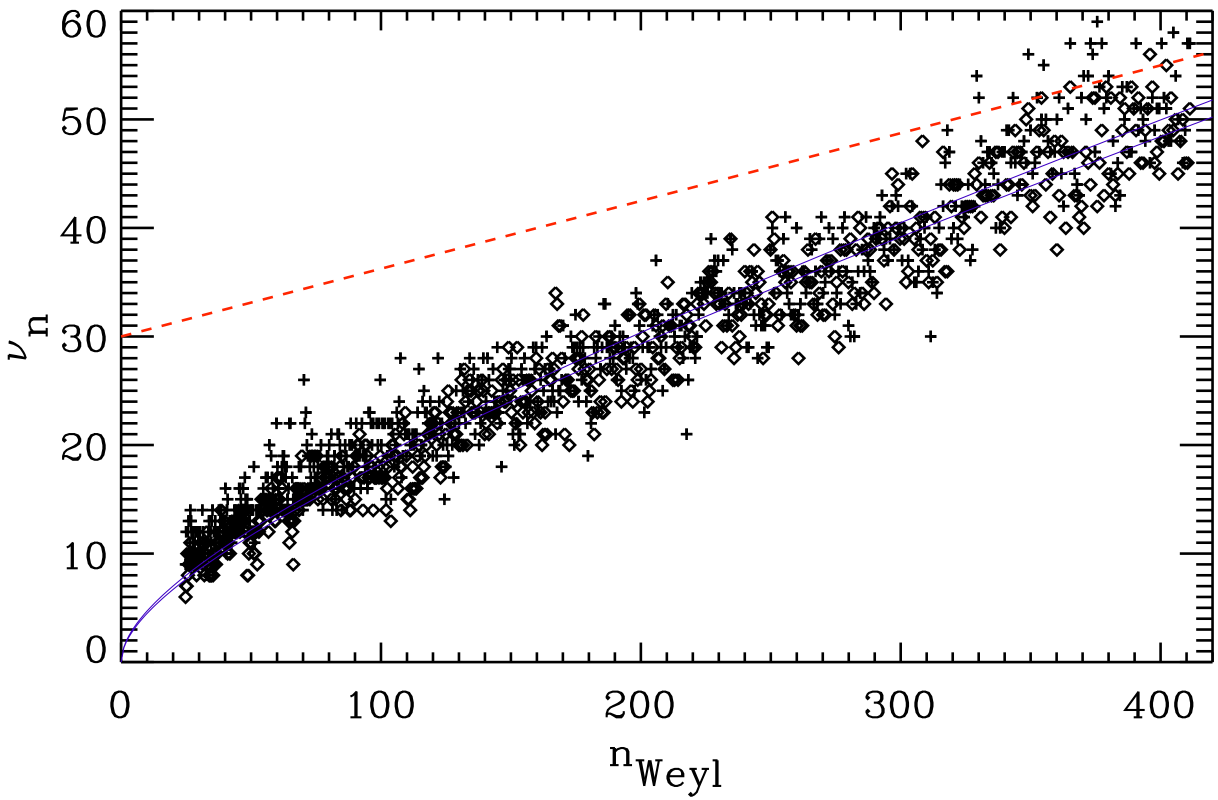

Number of nodal domains for real (+) and imaginary ($\diamond$) part

solid line:

$\nu_n = an + b\sqrt{n}$

$a = 0.059, b = 1.3$

Asymptotically in agreement with percolation model (- - -).

Area distribution of nodal domains

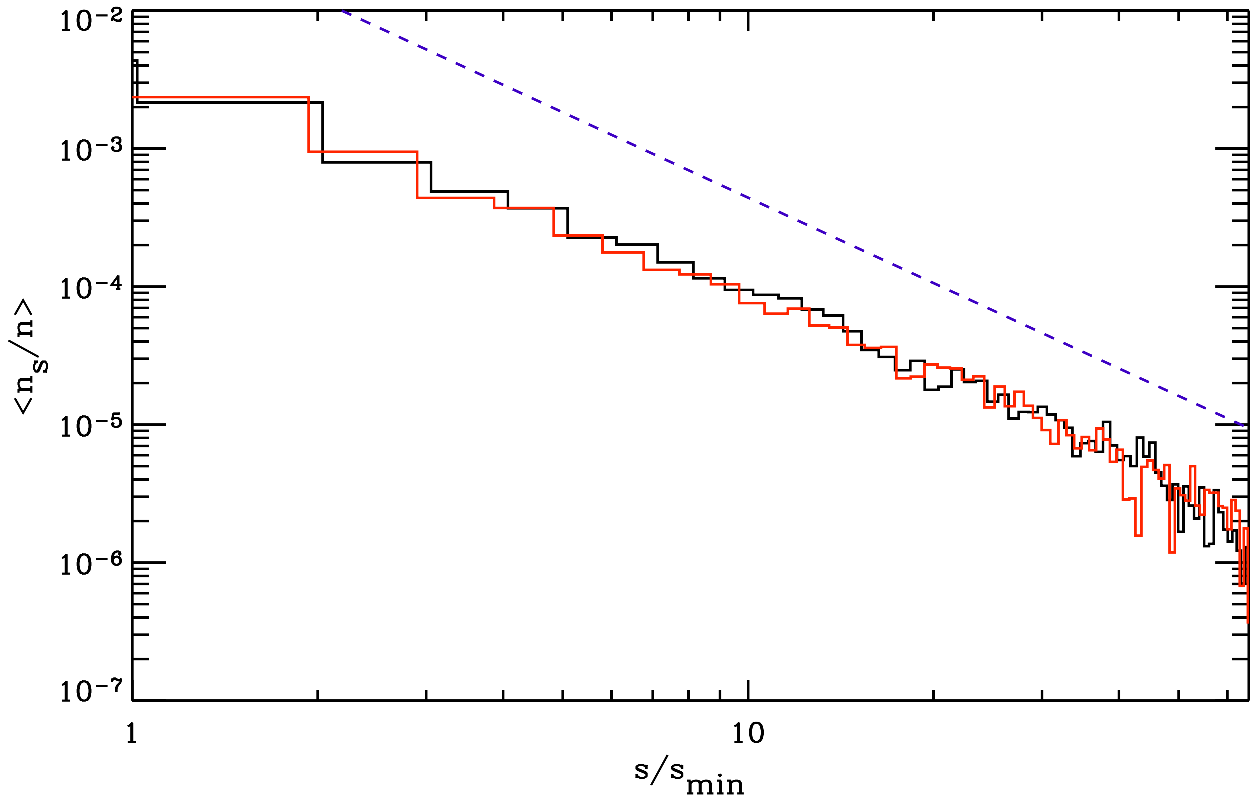

- Area distribution for the real and imaginary part
- Area normalized by $s_{\min} = \pi/(x_1 k)^2$, x_1: first zero of $J_0(x)$
- In agreement with expected algebraic decay of $(s/s_{\min})^{-187/91}$ from percolation model (shown as dashed line).

Random superposition of plane waves

Amplitude distributions

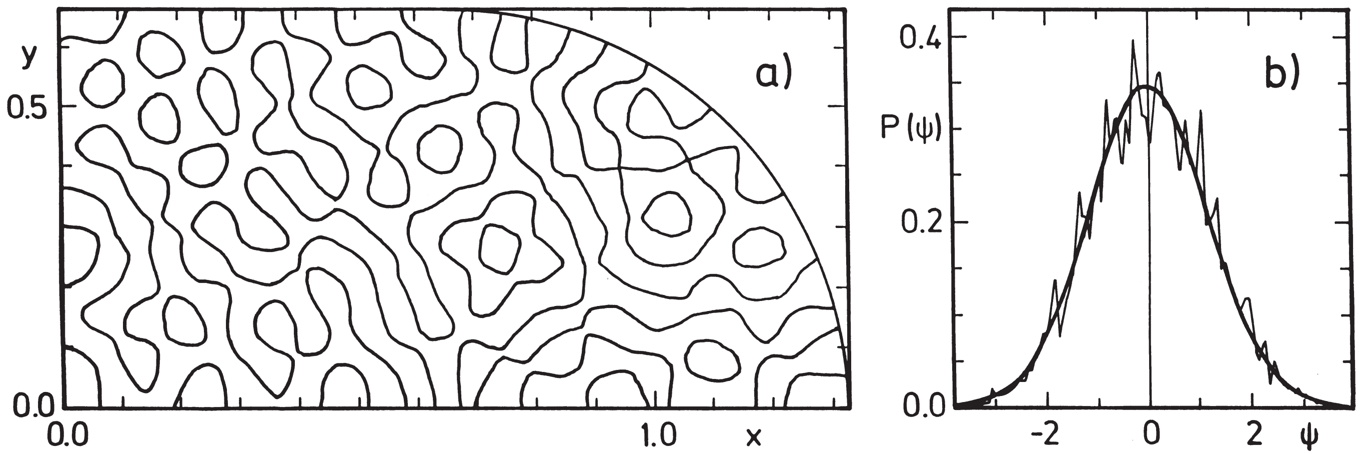

Observation:

Most wave function amplitudes in chaotic billiards are Gaussian distributed (McDonald, Kaufman 1979)

$$p(\psi) = \sqrt{\frac{A}{2\pi}} \exp\left(-\frac{A\psi^2}{2}\right) \qquad A\text{: billiard area}$$

Amplitude distributions (*cont.*)

For the squared amplitudes $\rho = |\psi|^2$ one obtains a Porter-Thomas distribution instead

$$p(\rho) = \sqrt{\frac{A}{2\pi\rho}} \exp\left(-\frac{A}{2}\rho\right)$$

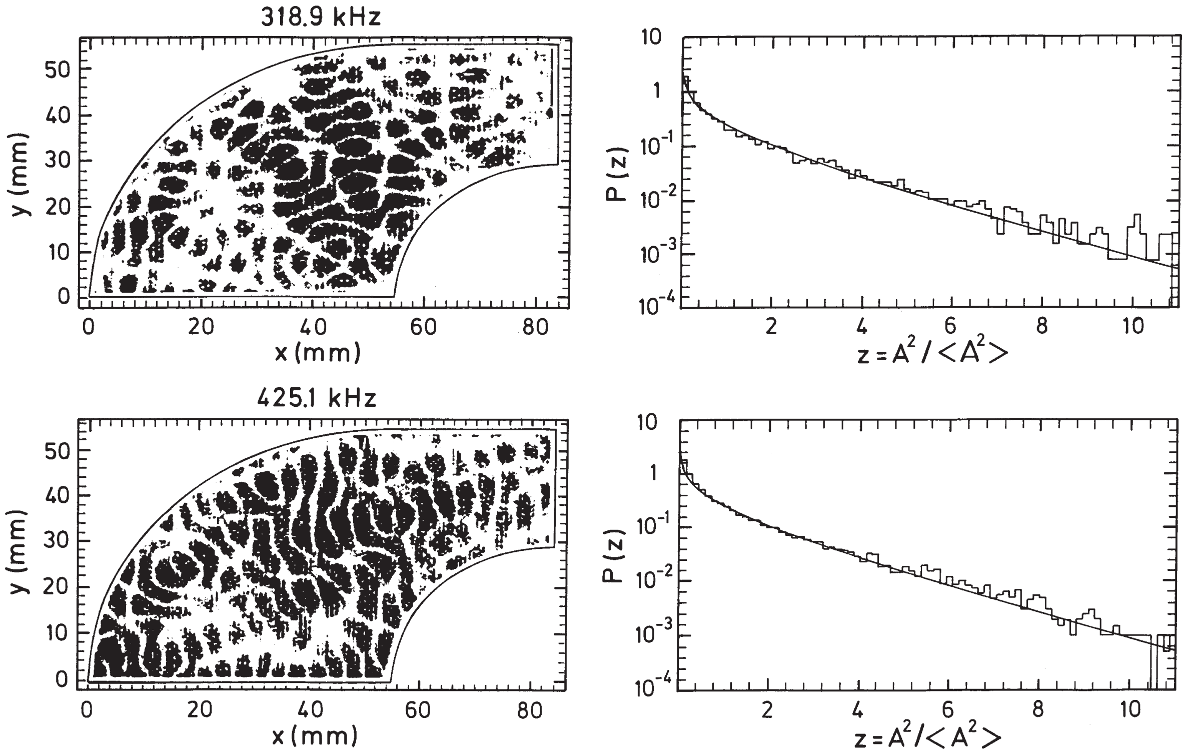

Example: Squared amplitude distribution of vibrating silicon plates (Schaadt 1997).

Berry's conjecture

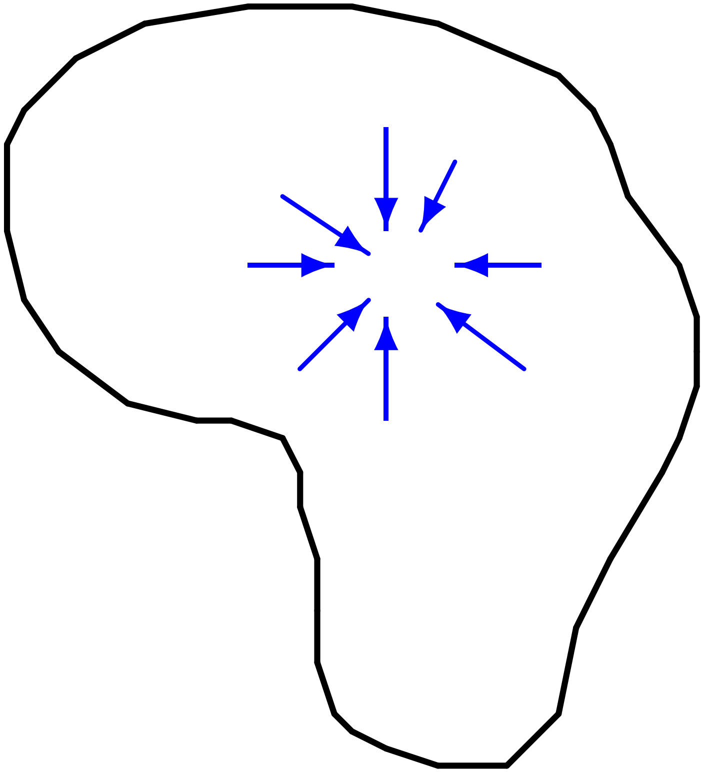

In a chaotic billiard at any site the wave function may be considered as a random superposition of plane waves (Berry 1977)

$$\psi(k, r) = \sum_n a_n e^{\imath k_n r}\,, \qquad |k_n| = k$$

The Gaussian distributions of the wave function amplitudes then follow immediately from the central-limit theorem.

Berry's conjecture

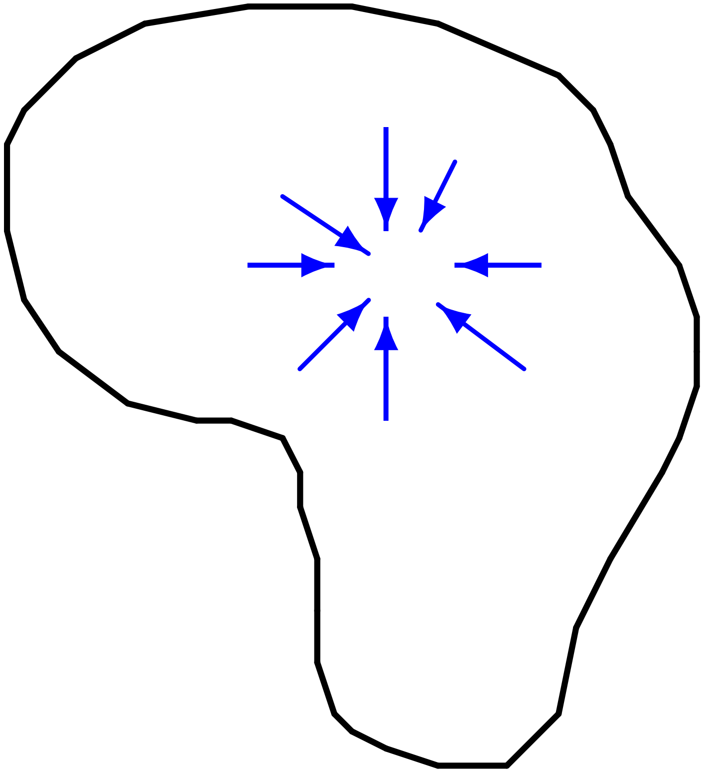

In a chaotic billiard at any site the wave function may be considered as a random superposition of plane waves (Berry 1977)

$$\psi(k,r) = \sum_n a_n e^{\imath k_n r}\,, \qquad |k_n| = k$$

The Gaussian distributions of the wave function amplitudes then follow immediately from the central-limit theorem.

The same model has been derived independently in acoustics (Ebeling 1978).

Light through distorted glas fibers

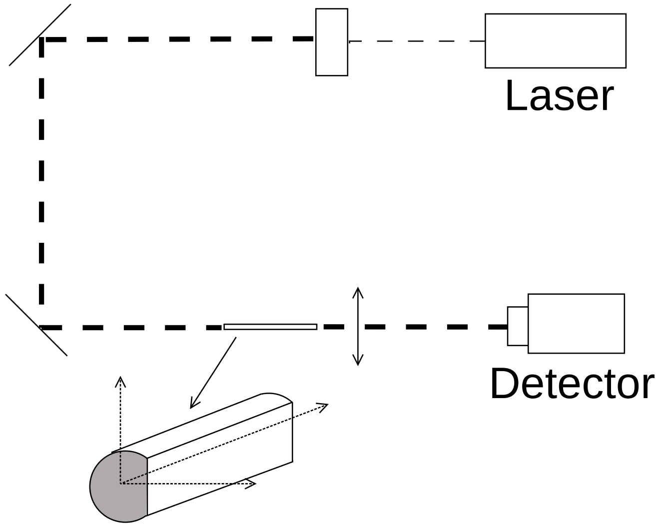

Example:

Monochromatic light, transported through a glas fiber with a D-shaped cross-section (Doya *et al.* 2002).

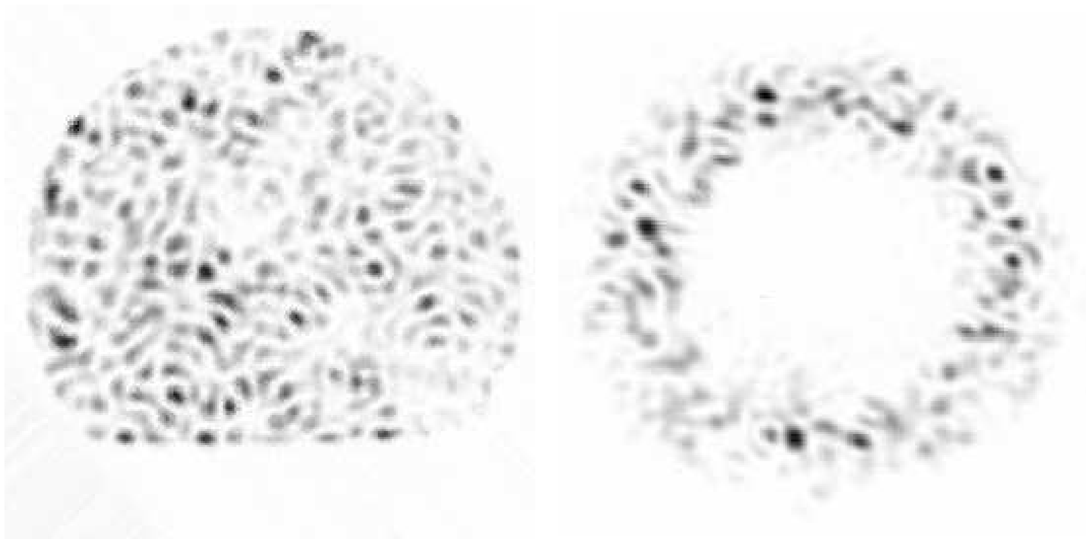

left: near-field intensity

right: far-field intensity ($\hat{=}$ Fourier transform of near-field intensity)

Spatial autocorrelation functions

Example: Amplitude spatial autocorrelation function

$C_\psi(\vec{r}) = \langle \psi^*(\vec{r} + \vec{r}_0)\psi(\vec{r}_0)\rangle$ $\quad\langle\cdots\rangle$: ensemble average

Spatial autocorrelation functions

Example: Amplitude spatial autocorrelation function

$C_\psi(\vec{r}) = \langle \psi^*(\vec{r} + \vec{r}_0)\psi(\vec{r}_0)\rangle$ $\langle \cdots \rangle$: ensemble average

With $\psi(\vec{r}) = \sum_n a_n e^{\imath \vec{k}_n \vec{r}}$ follows

$$\begin{aligned}
C_\psi(\vec{r}) &= \sum_{n,m} \langle a_n a_m^* e^{\imath\left[\vec{k}_n(\vec{r}+\vec{r}_0) - \vec{k}_m \vec{r}_0\right]}\rangle \\
&= \sum_n \langle |a_n|^2\rangle \langle e^{\imath \vec{k}_n \vec{r}}\rangle \\
&= \frac{1}{A}\langle e^{\imath k r \cos\phi}\rangle
\end{aligned}$$

or

$$C_\psi(\vec{r}) = \frac{1}{A} J_0(kr)\,, \qquad r = |\vec{r}|$$

Spatial autocorrelation functions

Example: Amplitude spatial autocorrelation function

$C_\psi(\vec{r}) = \langle \psi^*(\vec{r}+\vec{r}_0)\psi(\vec{r}_0)\rangle \qquad \langle\cdots\rangle$: ensemble average

With $\quad \psi(\vec{r}) = \sum_n a_n e^{\imath \vec{k}_n \vec{r}} \quad$ follows

$$
\begin{aligned}
C_\psi(\vec{r}) &= \sum_{n,m} \langle a_n a_m^* e^{\imath[\vec{k}_n(\vec{r}+\vec{r}_0)-\vec{k}_m\vec{r}_0]}\rangle \\
&= \sum_n \langle |a_n|^2\rangle\langle e^{\imath\vec{k}_n\vec{r}}\rangle \\
&= \frac{1}{A}\langle e^{\imath kr\cos\phi}\rangle
\end{aligned}
$$

or

$$C_\psi(\vec{r}) = \frac{1}{A}J_0(kr)\,, \qquad r = |\vec{r}|$$

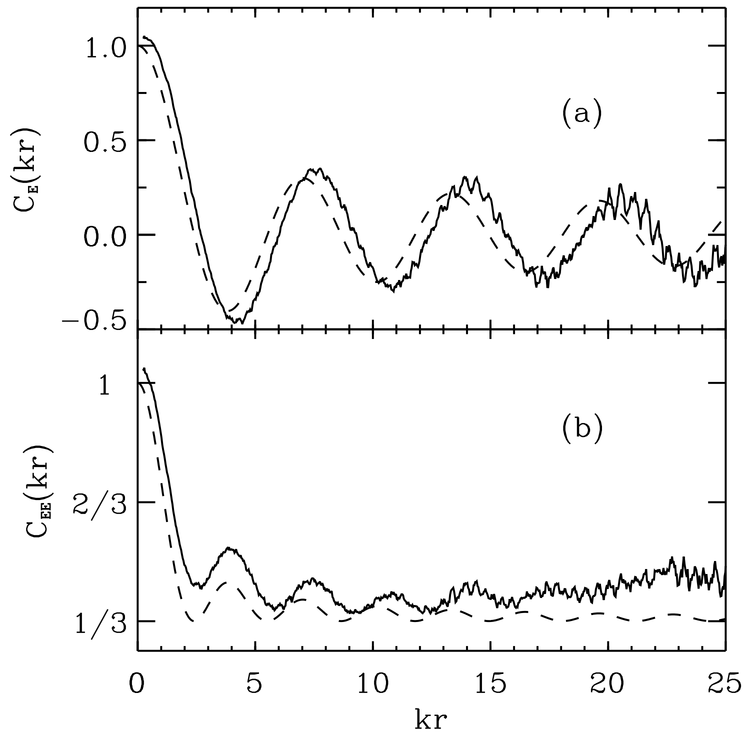

Spatial autocorrelation function for $\psi(r)$ (a) and $|\psi(r)|^2$ (b) in a 2D Sinai microwave billiard (Kim *et al.* 2003).

Justification of the model

Green function

$$G(\vec{r}_1, \vec{r}_2, E) = \sum_n \frac{\psi_n^*(\vec{r}_1)\psi_n(\vec{r}_2)}{E - E_n}$$

With

$$\delta(E) = \lim_{\varepsilon \to 0} \frac{1}{\pi} \frac{\varepsilon}{E^2 + \varepsilon^2} = -\frac{1}{\pi} \mathrm{Im} \frac{1}{E + \imath\varepsilon}$$

it follows

$$-\frac{1}{\pi} \mathrm{Im} G(\vec{r}_1, \vec{r}_2, E + \imath\varepsilon) = \sum_n \delta(E - E_n) \psi_n^*(\vec{r}_1) \psi_n(\vec{r}_2)$$

Justification of the model

Green function

$$G(\vec{r}_1, \vec{r}_2, E) = \sum_n \frac{\psi_n^*(\vec{r}_1)\psi_n(\vec{r}_2)}{E - E_n}$$

With

$$\delta(E) = \lim_{\varepsilon \to 0} \frac{1}{\pi} \frac{\varepsilon}{E^2 + \varepsilon^2} = -\frac{1}{\pi} \mathrm{Im} \frac{1}{E + \imath\varepsilon}$$

it follows

$$-\frac{1}{\pi} \mathrm{Im} G(\vec{r}_1, \vec{r}_2, E + \imath\varepsilon) = \sum_n \delta(E - E_n) \psi_n^*(\vec{r}_1)\psi_n(\vec{r}_2)$$

$\Longrightarrow$

$$-\frac{1}{\pi} \langle \mathrm{Im} G(\vec{r}_1, \vec{r}_2, E + \imath\varepsilon) \rangle_E = \rho(E) \langle \psi_n^*(\vec{r}_1)\psi_n(\vec{r}_2) \rangle_E$$

where $\rho(E) = \frac{A}{4\pi}$ for 2D billiards (Weyl formula).

Justification of the model (*cont.*)

Far off the walls the Green function can be replaced by the free-particle Green function

$$G(\vec{r}_1, \vec{r}_2, E) \approx -\frac{\imath}{4} H_0^{(1)}\left(k\left|\vec{r}_1 - \vec{r}_2\right|\right), \qquad E = k^2$$

$\Longrightarrow$

$$\begin{aligned}
\langle \psi_n^*(\vec{r}_1)\psi_n(\vec{r}_2)\rangle_E &= -\frac{1}{\pi\rho(E)}\langle \mathrm{Im} G(\vec{r}_1, \vec{r}_2, E + \imath\varepsilon)\rangle_E \\
&= \frac{1}{4\pi\rho(E)}\langle \mathrm{Re} H_0^{(1)}\left(k\left|\vec{r}_1 - \vec{r}_2\right|\right)\rangle_E \\
&= \frac{1}{A} J_0\left(k\left|\vec{r}_1 - \vec{r}_2\right|\right)
\end{aligned}$$

in accordance with our previous result (Hortikar *et al.* 2002, Urbina *et al.* 2003)!

Justification of the model (*cont.*)

Far off the walls the Green function can be replaced by the free-particle Green function

$$G(\vec{r}_1, \vec{r}_2, E) \approx -\frac{\imath}{4} H_0^{(1)}\left(k\,|\vec{r}_1 - \vec{r}_2|\right)\,, \qquad E = k^2$$

$\Longrightarrow$

$$\begin{aligned}
\langle \psi_n^*(\vec{r}_1)\psi_n(\vec{r}_2)\rangle_E &= -\frac{1}{\pi\rho(E)}\langle \mathrm{Im} G(\vec{r}_1, \vec{r}_2, E + \imath\varepsilon)\rangle_E \\
&= \frac{1}{4\pi\rho(E)}\langle \mathrm{Re} H_0^{(1)}\left(k\,|\vec{r}_1 - \vec{r}_2|\right)\rangle_E \\
&= \frac{1}{A} J_0\left(k\,|\vec{r}_1 - \vec{r}_2|\right)
\end{aligned}$$

in accordance with our previous result (Hortikar *et al.* 2002, Urbina *et al.* 2003)!

However: Now the average is over all wave functions within an energy window, no longer over individual wave functions!

Flows

Wave functions

Open system or system with broken time reversal symmetry:

$$\psi = \psi_R + \imath\psi_I = |\psi| \exp(\imath\phi)$$

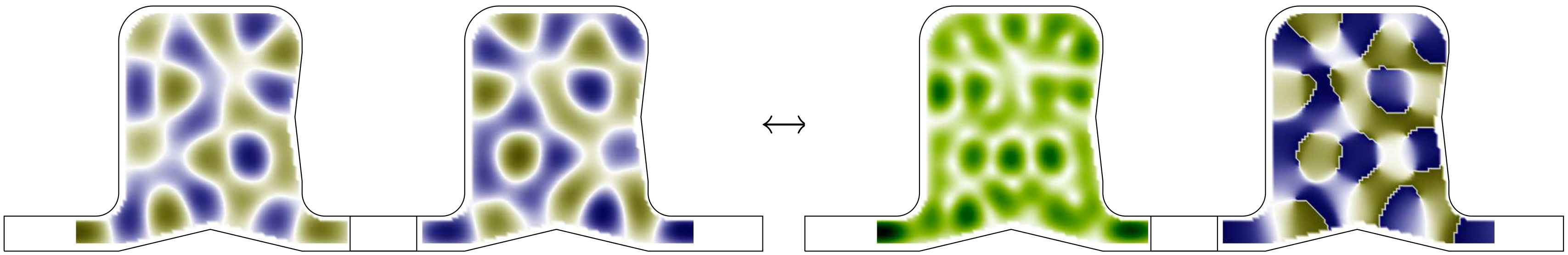

Wave functions

Open system or system with broken time reversal symmetry:

$$\psi = \psi_R + \imath\psi_I = |\psi| \exp(\imath\phi)$$

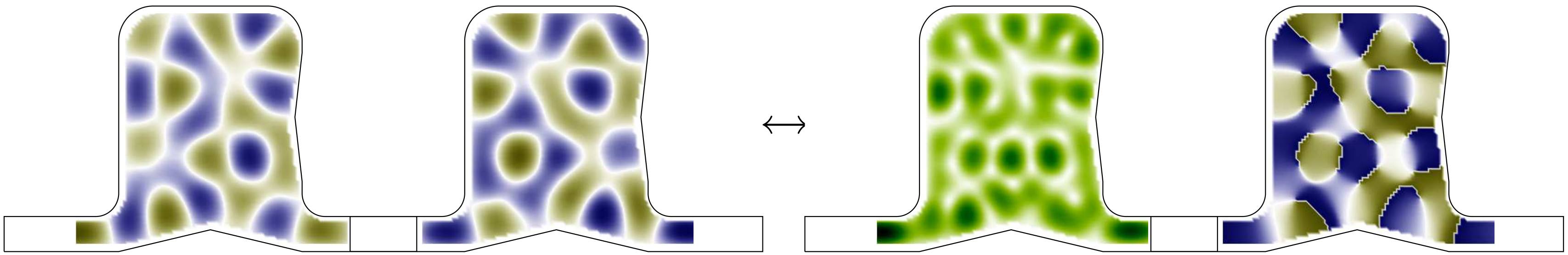

Additionally there is a flow of energy:

from	E_z	$\hat{=}$	ψ
follows	$\vec{S} \propto \frac{c}{4\pi}\mathrm{Im}\left[E_z^* \nabla E_z\right]$	$\hat{=}$	$\vec{j} = \frac{\hbar}{m}\mathrm{Im}\left[\psi^* \nabla \psi\right]$
	Poynting vector		Current density

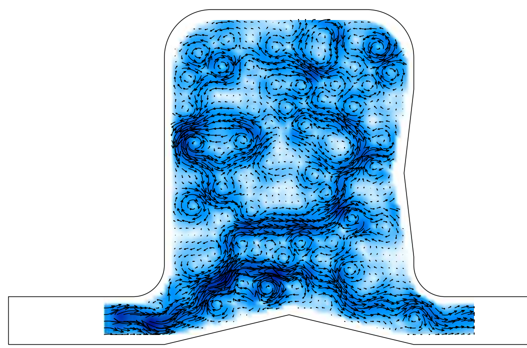

Vortices and saddles

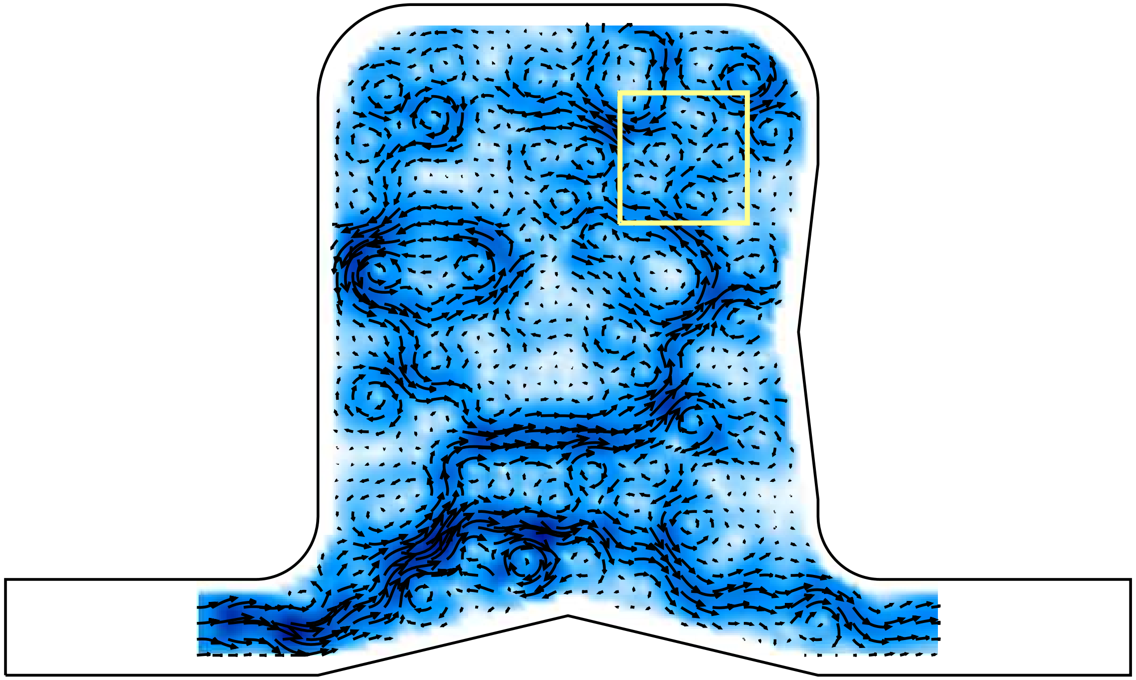

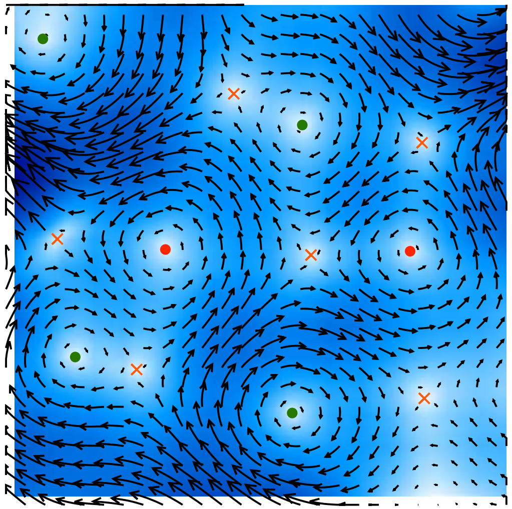

vortex: clockwise (+): ● counterclockwise (-): ●

saddles: orange crosses ×

Nearest neighbour distances

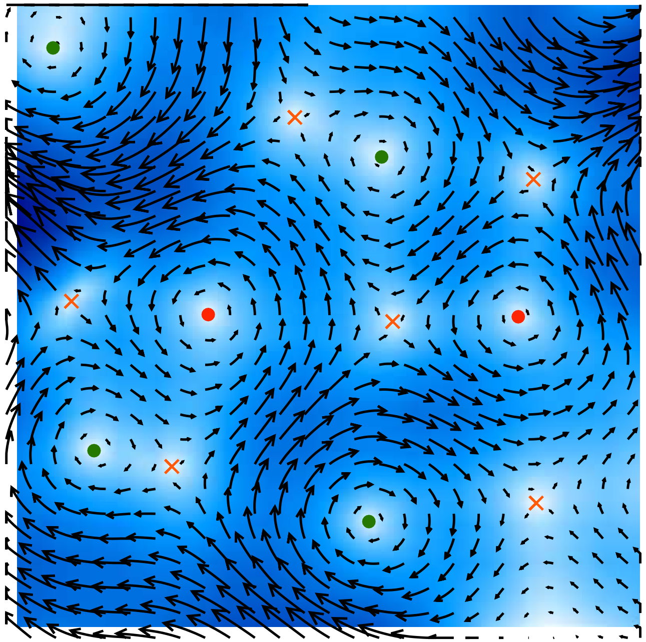

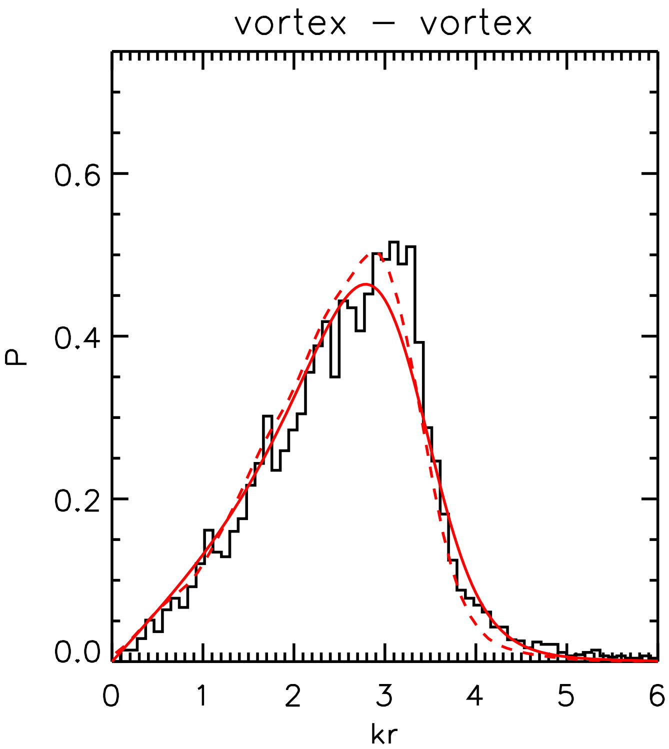

- Solid lines show analytical results in Poisson approximation [Saichev et. al., 2001].
- Dashed lines numerical results of the random plane wave model
- Good agreement between theory and experiment

Pair correlation functions

g: pair correlation function

g_Q: charge correlation function

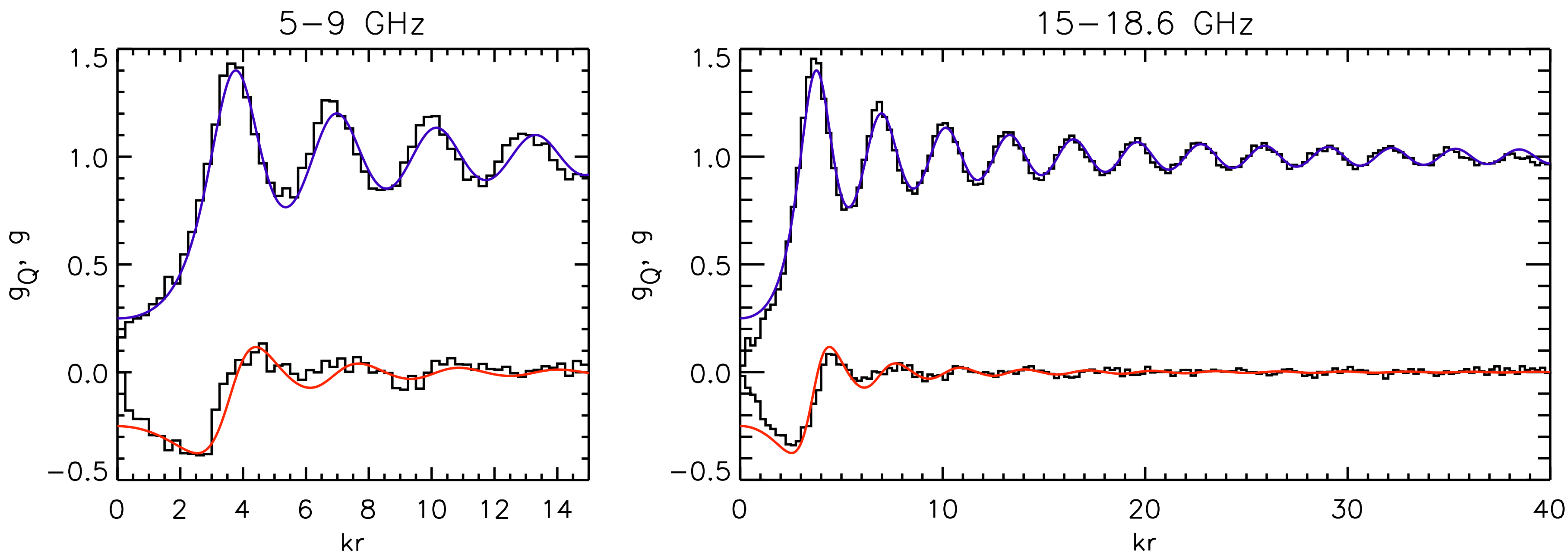

- Good agreement for small kr but period length to small
- Very good agreement, only for lower kr small deviations

[Berry, Dennis 2000; Saichev et. al. 2001; Bäcker, Schubert 2002]

Limitations of the model

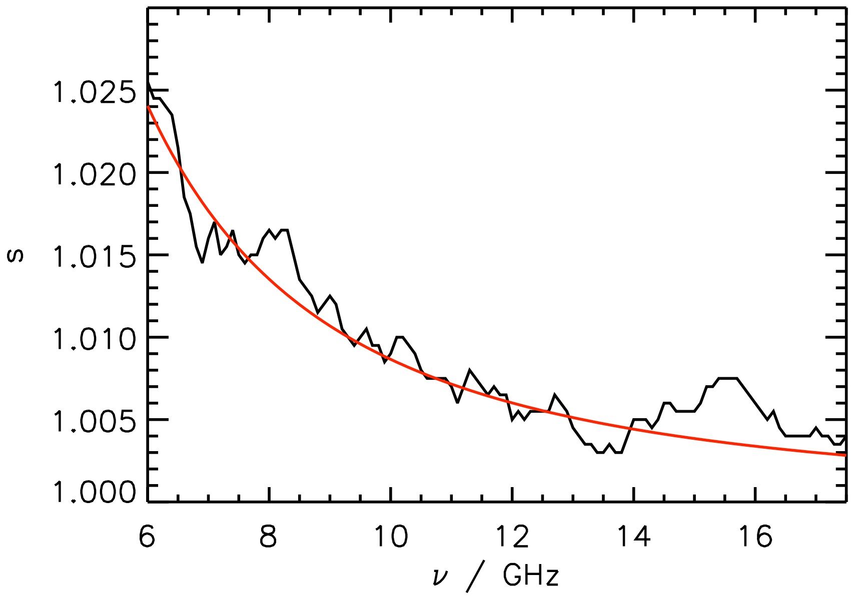

Stretching factor s needed to adjust the experimentally observed oscillations to theory

Explanation: For wavelengths comparable to the system size L the frequencies of the plane waves are smeared out over a window of width $\delta \sim L^{-1}$.

This leads to a stretching and damping of the correlation functions:

$$g(kr) \to g(skr)e^{-\frac{\delta^2 r^2}{2}}$$

Derivation of the stretching factor

All correlation functions are oscillatory with an algebraic damping

$$g(x) = e^{-a(kx)} \cos(kx)\,, \qquad a(kx) = n \ln(kx)$$

Convolution by a Gaussian function yields

$$g_{\rm conv}(x) = \Re \left[\frac{1}{\sqrt{\pi}\delta} \int d\bar{k} e^{-a(\bar{k}x) - \imath \bar{k}x - \frac{(\bar{k}-k)^2}{2\delta^2}} \right]$$

Expanding $a(\bar{k}x)$ up to the linear term at $\bar{k} = k$ one gets

$$g_{\rm conv}(x) = e^{-a(kx)} \cos(skx) e^{-\frac{\delta^2 x^2}{2}}$$

where

$$s = 1 + \frac{\delta^2 x}{k} a'(kx) = 1 + n \left(\frac{\delta}{k}\right)^2$$

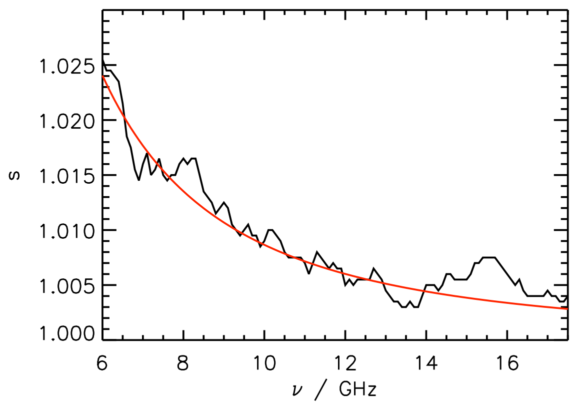

Another example

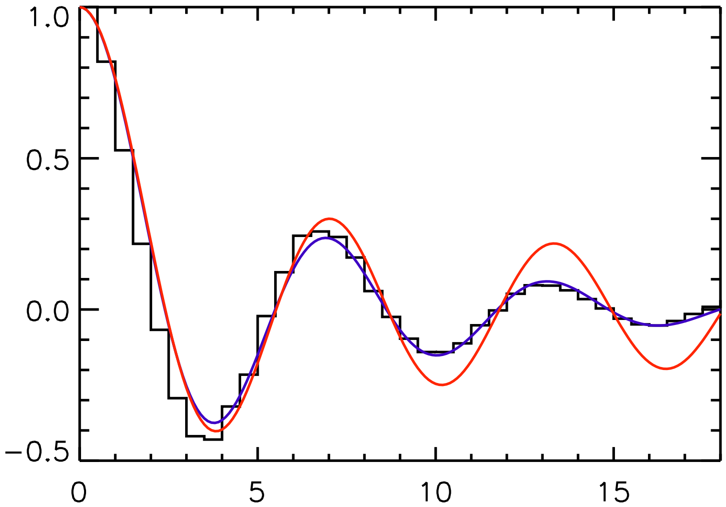

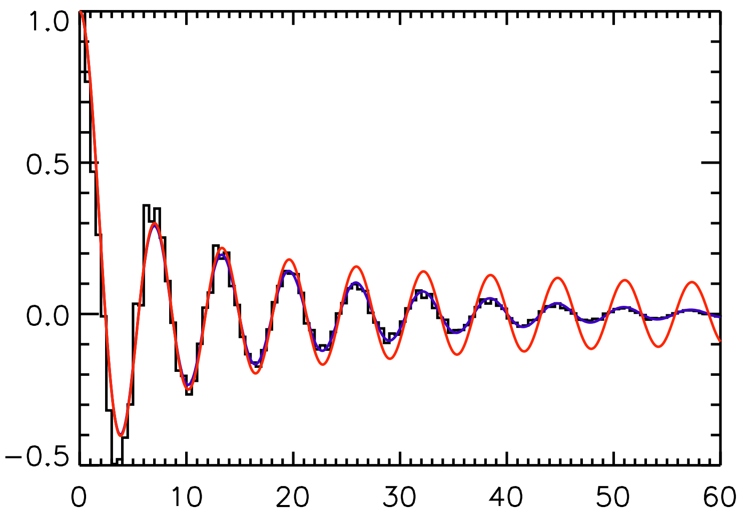

Spatial amplitude autocorrelation function in the low (top) and high (bottom) frequency regime

—: random plane wave model without
—: and with stretching corrections

Freak waves

Motivation

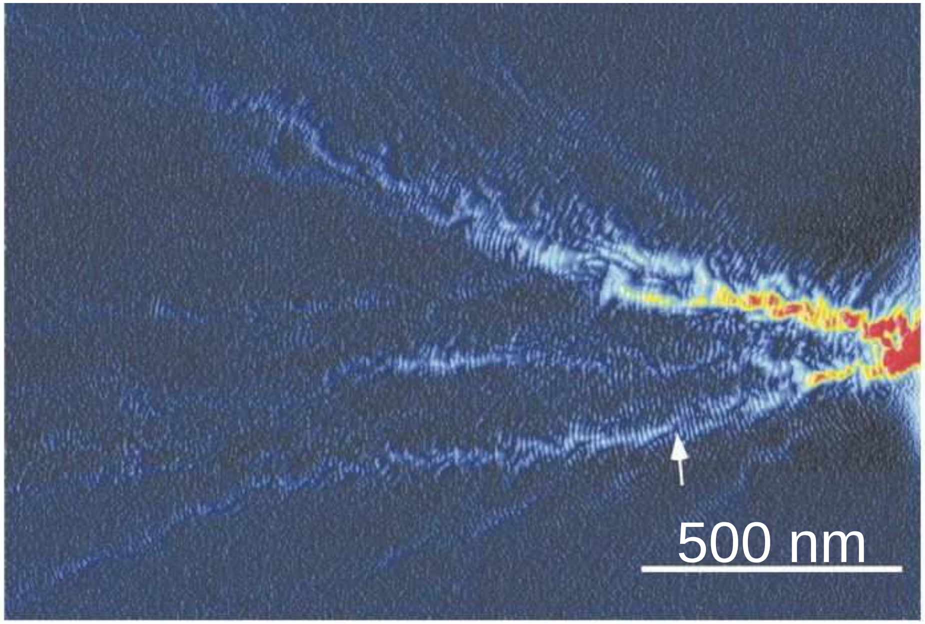

STM measurements of electron flow through quantum point contact show fractal-like branch structures (Topinka *et al.* 2001)

Conjecture (Kaplan 2002): Branches are caused by caustics in a potential landscape with a Gaussian correlated potential:

$$\overline{V(r)V(r')} \sim e^{-|r-r'|^2/\sigma^2}$$

If this is true, the branches should follow the slope, not the valleys, of the potential!

Experiment

For resonators with top and bottom parallel to each other with distance d, the z dependence of E can be separated,

$$E(x,y,z) = E(x,y)\cos\left(\frac{n\pi}{d}z\right)$$

It follows

$$\left[-\left(\frac{\partial^2}{\partial x^2}+\frac{\partial^2}{\partial y^2}\right)+\left(\frac{n\pi}{d}\right)^2\right]E(x,y) = k^2E(x,y)$$

$n=0$: hard-wall reflection
$n\neq 0$: additional term can be used to mimic a potential (Lauber *et al.* 1994):

$$V(x,y) = \left[\frac{n\pi}{d(x,y)}\right]^2$$

Condition: height variation must be adiabatic!

Set-up

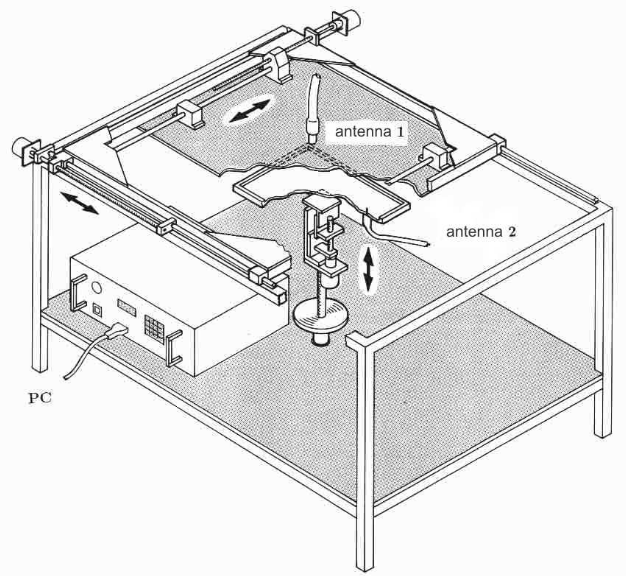

Transmission measured between fixed antenna in the bottom, and movable antenna in the top

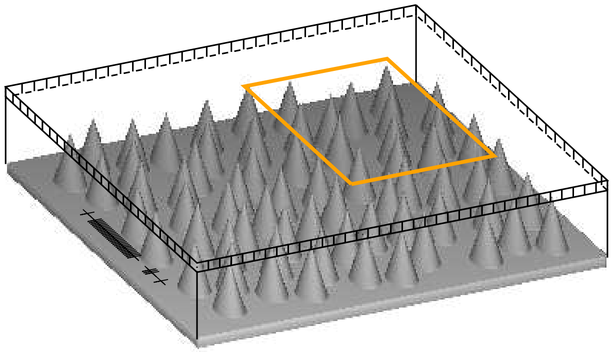

Arrangement of randomly distributed cones ($R = 2.5$ mm, $H = 10$ mm) mimicking a potential

$$V(\vec{r}) = \frac{(\pi n)^2}{\left(h_{\min} + \frac{H}{R}|\vec{r}|\right)^2}$$

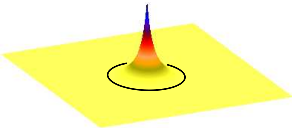

$h_{\min}$: distance between cone tip and top plate

Stationary field distributions

$\nu = 31\,$GHz:

five propagating modes n=0,. . . 4

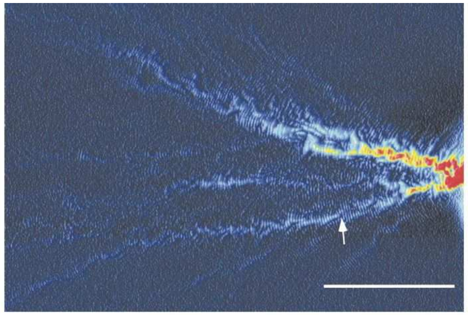

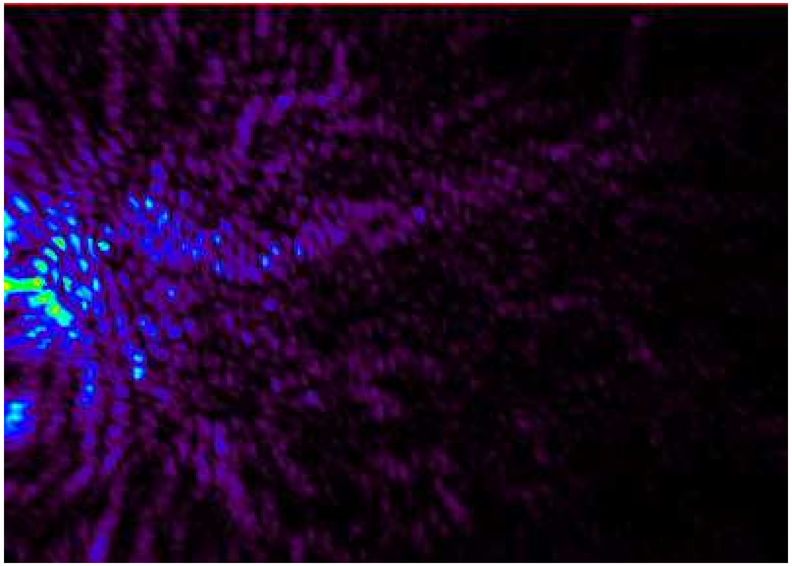

Experiment

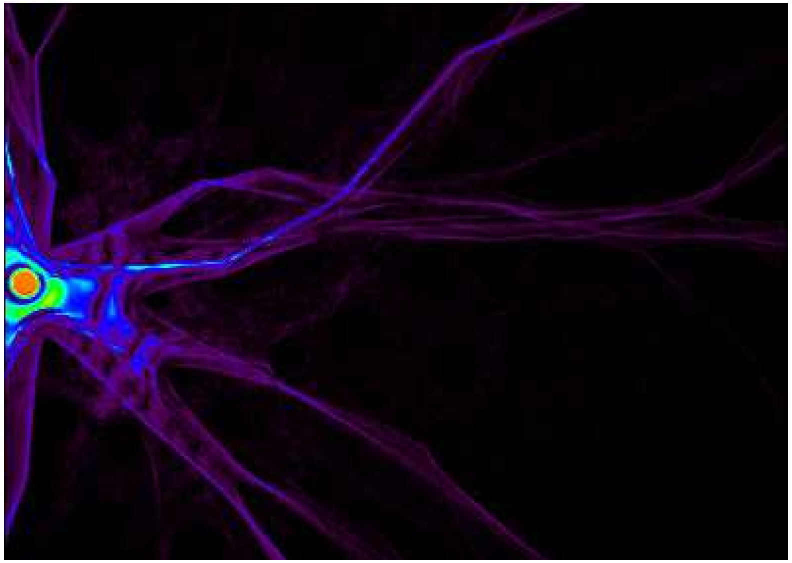

Simulation

Stationary field distributions

$\nu = 31$ GHz:

five propagating modes n=0,. . . 4

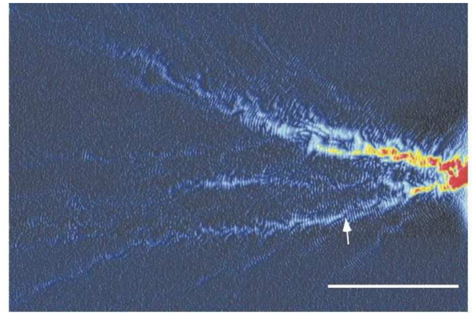

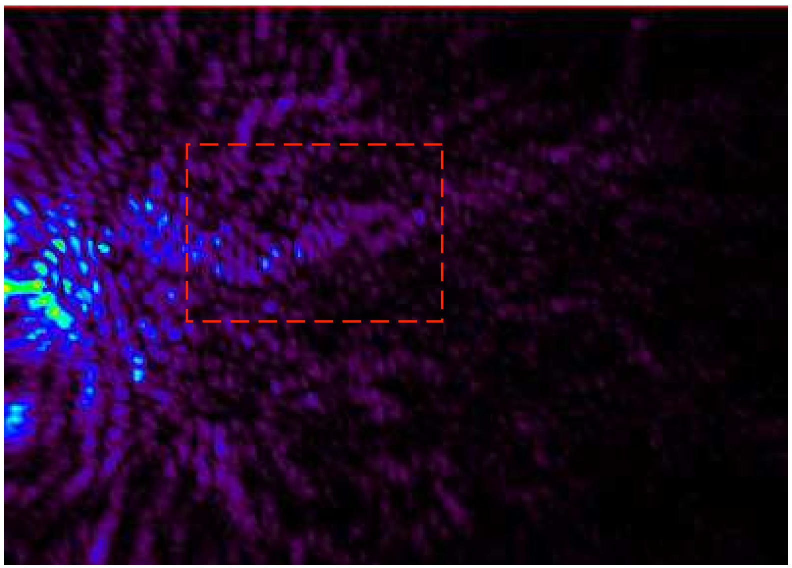

Experiment

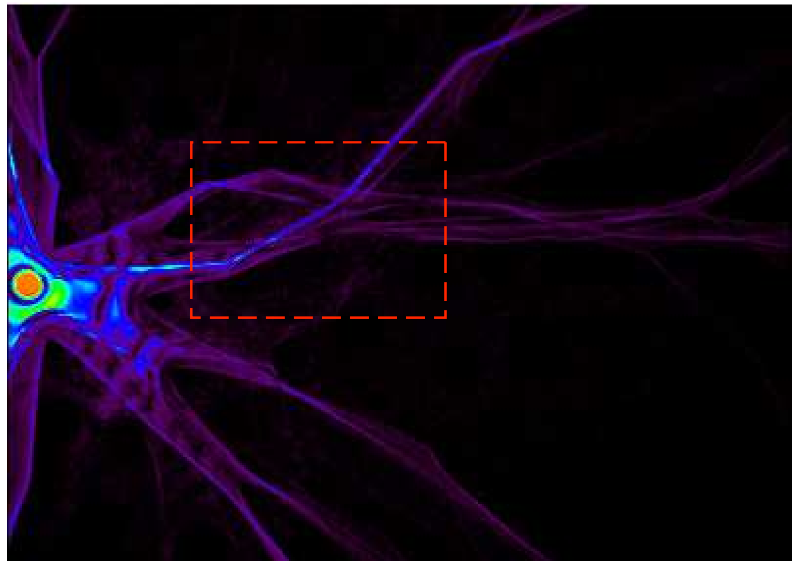

Simulation

Stationary field distributions (*cont.*)

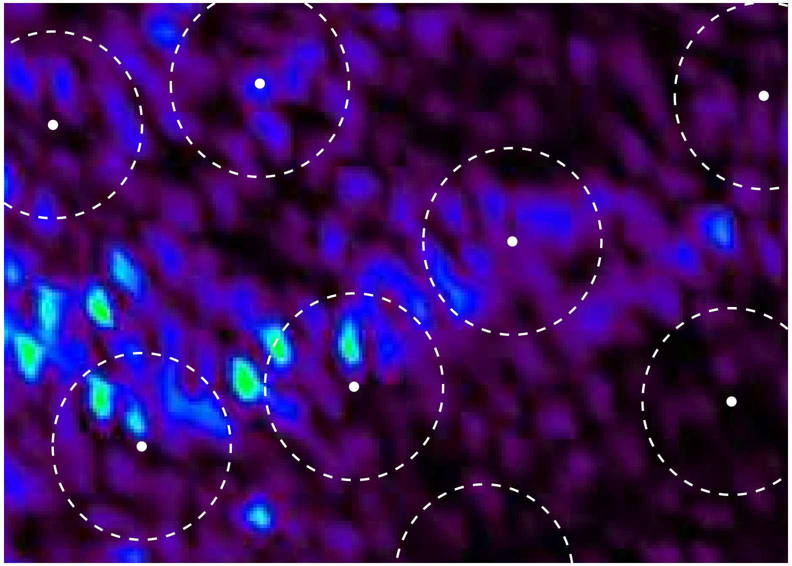

Experiment

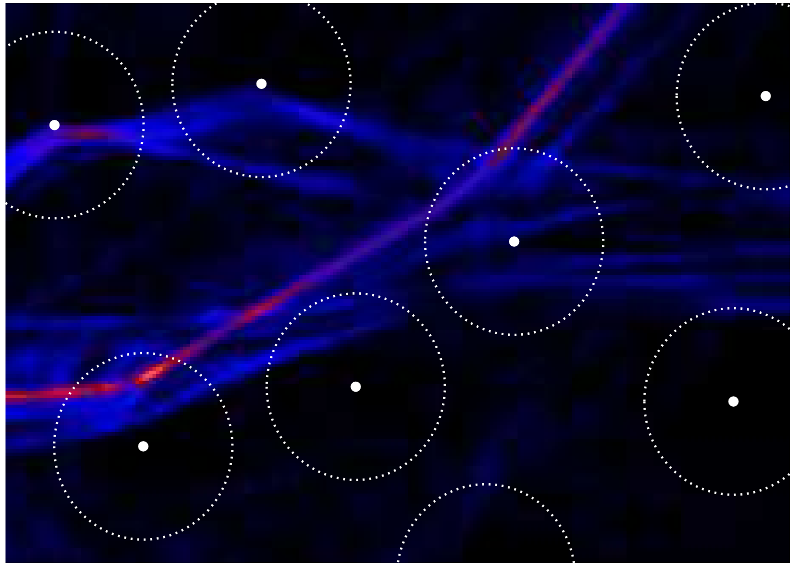

Simulation

Caustics are responsible!

Relation to waves in the sea

The approach of Gaussian correlated potential may be applied to many other situations as well, such as

- light propagation in media with varying index of refraction
- Evolution of wave patterns in spatially varying velocity fields

This allows a reinterpretation of the microwave results to study, e. g.,

- Tsunami amplification by potential landscapes in shallow water (Dobrokhotov *et al.* 2006, Berry 2007)
- Formation of freakwaves due to eddy-generated local velocity fields (Heller *et al.* 2008)

Freak waves

Random superposition of plane waves yields

$$p(H) \sim e^{-H^2/2\sigma^2} \qquad \text{(Rayleigh's law)}$$

for probability to find a wave with height $> H$ above sealevel.

The actual number found in observations is much higher!

The hot spots

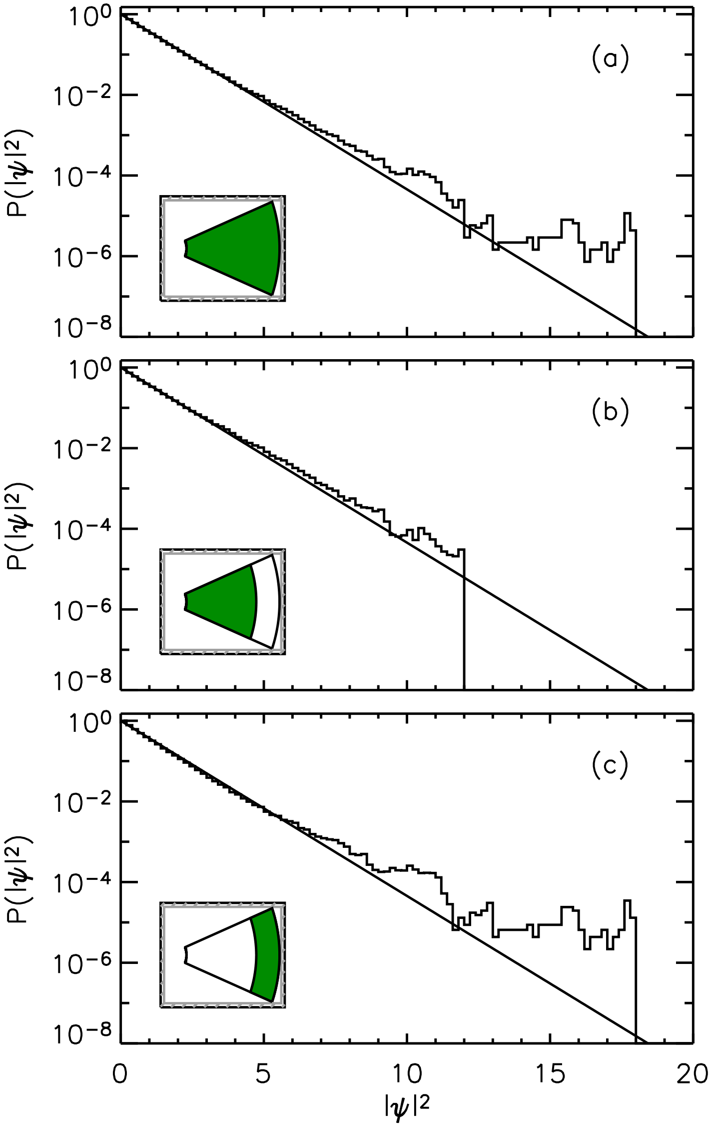

Random expectation:

$$p(I) = \frac{1}{\langle I \rangle} e^{-I/\langle I \rangle}\,, \quad I = |\psi|^2$$

The hot spots

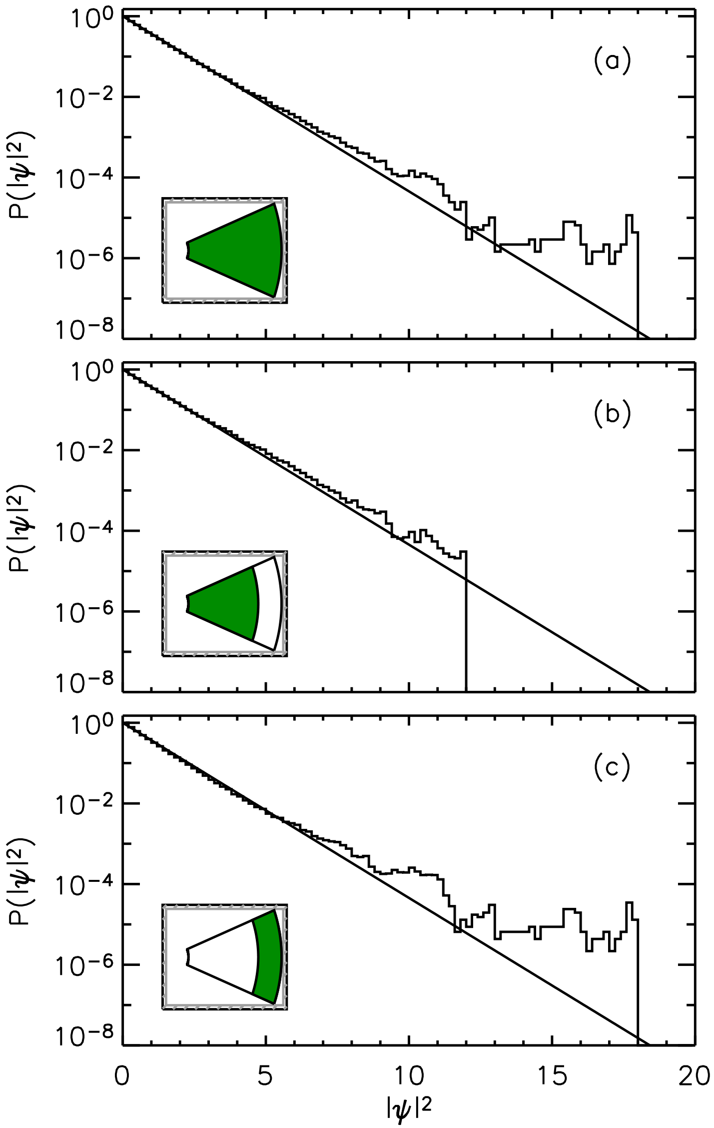

Random expectation:

$$p(I) = \frac{1}{\langle I \rangle} e^{-I/\langle I \rangle}\,, \quad I = |\psi|^2$$

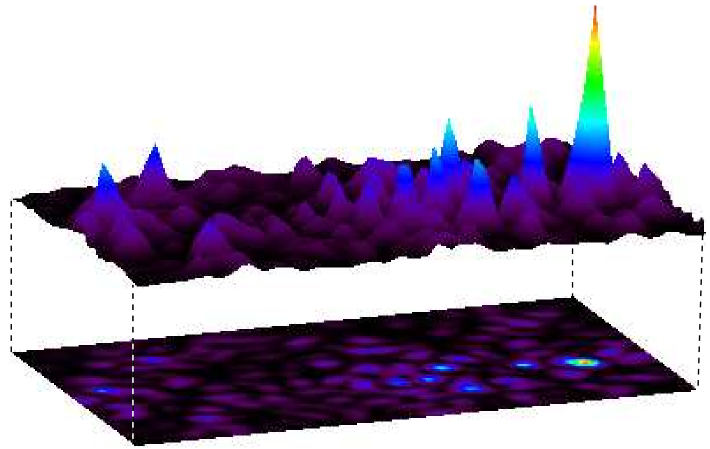

"Hot spots", observed in all scattering arrangement within limited frequency windows ($\Delta\nu \approx 0.5$ GHz).

Second order caustics effects?

Transient behavior

Pulse generation, by superimposing wave functions from a Gaussian frequency window about a hot spot, entering from different antenna positions x_i:

$$\psi(\vec{r},t) = \frac{1}{N}\sum_{i=1}^{N} \psi_{x_i}(\vec{r},\omega_i) e^{\imath(\omega_i t - \varphi_i)}$$

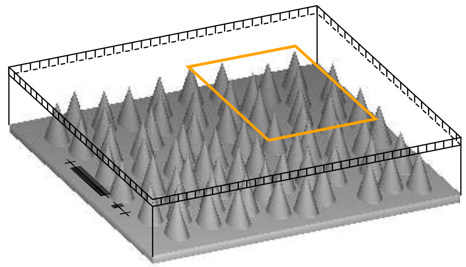

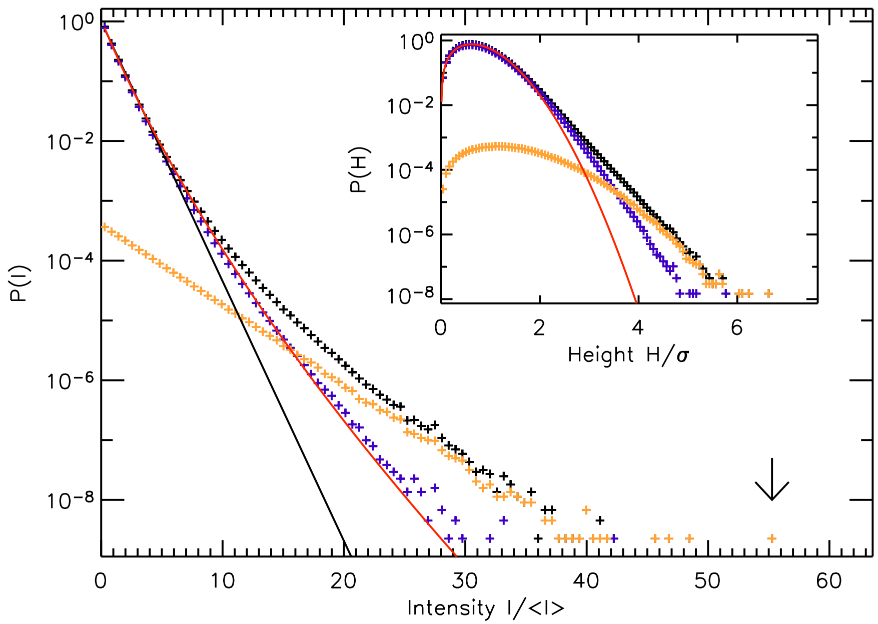

black: all points
orange: only hot spot
blue: all but hot spot region

solid black line: random expectation

Our super freak event

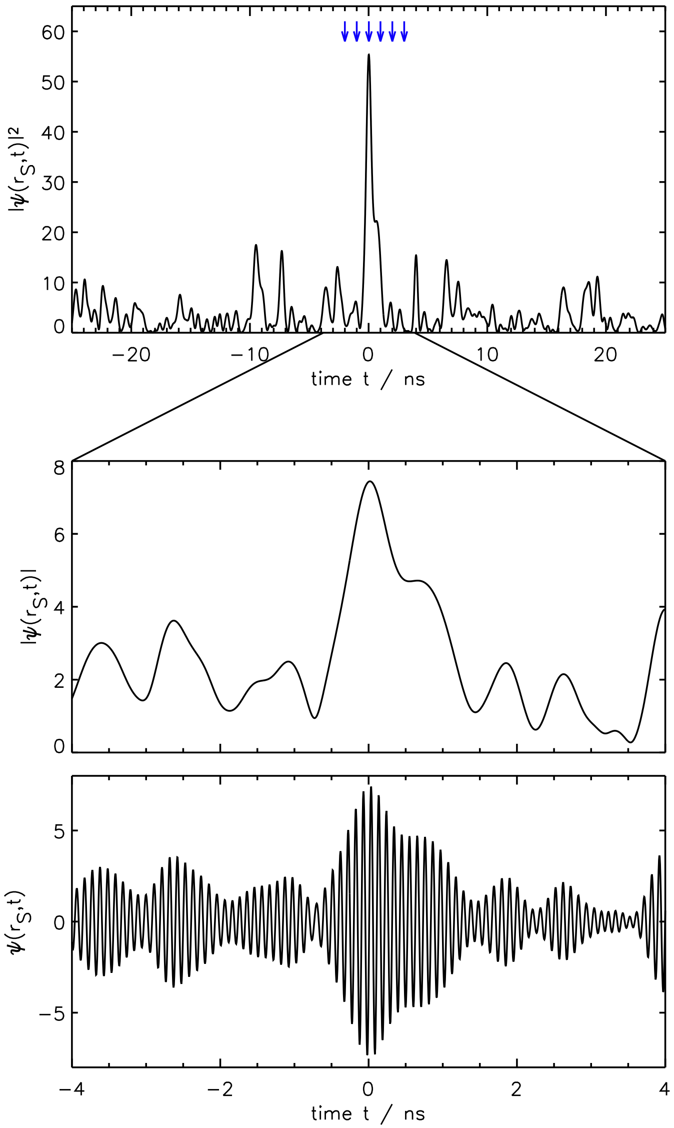

Intensity $I/\langle I\rangle = 55$

Experimental probability :10^{-9}

“rare”, but 15 (!) orders of magnitude larger as expected from a random superposition!

(c)

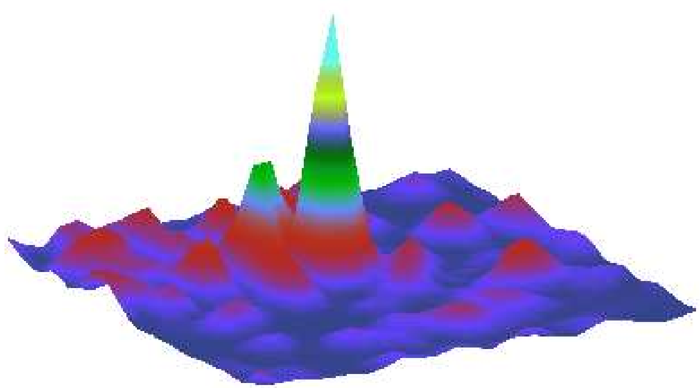

Summary

- Microwave techniques offer the unique possibility to test theories on the statistical properties of waves in chaotic systems.
- The percolation model is able to explain the statistical features of nodal domains
- The random plane wave model is able to explain
  - distribution of wave functions and currents
  - spatial correlations of wave functions and currents
  - two-point correlation function of vortex-vortex, etc.
- Limitations of the model close to boundaries are well understood
- Noticeable deviations in the presence of potential landscapes
- Implication for the understanding of the formation of rogue waves in the sea.

Thanks!

Coworkers:

U. Kuhl
M. Barth
K. Young-Hee
R. Schäfer
R. Höhmann

Cooperations:

S. Gnutzmann, Berlin
M. Dennis, Bristol, UK
J.-D. Urbina, Bogota, Colombia
E. Heller, Cambridge, USA
L. Kaplan, New Orleans, USA

The experiments have been supported by the DFG via the

FG 760 “Scattering Systems with Complex Dynamics”.